75th International Astronautical Congress (IAC), Milan, Italy, 14-18 October 2024.

IAC-24,A6,7,5,x84147

Early stage characterization of on-orbit fragmentation events

Paola Grattagliano[a*], Alessandro Mignocchi[a], Marco Felice Montaruli[a], Pierluigi Di Lizia[a], Alessandra Di Cecco[b], Marco M. Castronuovo[b]

[a]*Politecnico di Milano, Aerospace Science and Technology Department, via La Masa, 34, 20156 Milano, Italy*
[b]*Agenzia Spaziale Italiana (ASI), Via del Politecnico snc, 00133, Rome, Italy*
[*]Corresponding Author: paola.grattagliano@polimi.it

Abstract

The ongoing rise in the number of orbiting objects is a significant concern in the advancement of space services, posing a great threat to future missions and active satellites. Currently, fragmentation events are the dominant source of space debris, making the Fragmentation Analysis one of the main Space Surveillance and Tracking activities in supporting operators in the space traffic management. Prompt characterization of these break-up events is of paramount importance to achieve fast and accurate forecast of the fragments trajectories. Accomplishing this task implies two essential activities: associating a detected object to the fragmentation event and detecting the event epoch. To this end, a stochastic approach is considered fundamental to act operationally in the period immediately after a fragmentation, when the data are uncertain and scarce.
Concerning the association problem, the Orbital Parameters Intersection Analysis (OPIA) algorithm performs the Chi-Squared test, based on the Mahalanobis Distance, to assess the statistical matching between two distributions found in the RAAN-inclination plane, derived from the last available ephemeris of the parent and from the measurement track of the observed object. The latter is obtained through the admissible region concept, and this allows to apply the approach from a single measurement track and without an Initial Orbit Determination (IOD) result.
When the result of an IOD process is available for a single fragment, a novel version of the FRagmentation Epoch Detector (FRED) algorithm, based on typical tools of Conjunction Analysis, can be exploited. The proposed approach applies Gaussian Mixture Models (GMM) throughout the process to describe and propagate the parent and fragment state uncertainties. The algorithm computes a set of candidate fragmentation epochs, and then ranks them through the Probability of Collision (PoC) metric, to determine the best estimate of the event epoch. The computation of the PoC is also exploited to verify the association of a detected object to the event.
Both OPIA and FRED performance are tested in a realistic simulated scenario. Concerning OPIA, the simulations demonstrate satisfying accuracy, allowing an accurate event characterization even when the fragmentation epoch is not yet available. Regarding FRED, its robustness to increasing Orbit Determination (OD) errors and presence of dynamical perturbation is verified as well. At the expense of a slight increase in the sensitivity to state uncertainties, the upgraded version of FRED benefits from the GMM-based approach, which evidently reduces the computational effort.

Keywords: Space Debris, Space Surveillance and Tracking, Fragmentation events, TDMs, Admissible Regions, Conjunction Analysis.

1. Introduction

The ongoing rise in the number of Resident Space Objects (RSOs) in orbit is a significant concern in the advancement of space services, particularly within the Low Earth environment. The latest data regarding the amount of non-functioning orbiting objects are provided by ESA Space Debris Office. About 18,400 satellites have been placed into Earth orbit in more than 60 years of activities, causing now the presence of 40,500 debris with dimensions over 10 cm, 1,100,000 debris with dimensions between 1 cm and 10 cm and 130 million debris with smaller dimensions [1]. This population poses a great threat to both future and current missions. To address these challenges, different activities are carried out with the aim of cataloguing and characterizing the orbits of RSOs, monitoring the fragmentation events, and applying countermeasures to the problem. At European level, two major Space Surveillance and Tracking (SST) capabilities exist: the ESA Space Debris Office and the EUSST Consortium. Operations run by the latter are structured around three main functions: the sensor function, consisting of a network of ground-based sensors to survey and track space objects [2] [3] [4] [5] [6] [7] [8] [9] [10] [11]; a processing function, processing and analyzing SST data at national level to produce SST information and SST services [12]; and a service function providing SST services to the EU

user community [13]. The first one is the Collision Avoidance service, which provides risk assessment of collision, and generates collision avoidance alerts [14]. The second consists in the Re-entry Analysis, which provides risk assessment of uncontrolled re-entry of man-made space objects into the Earth's atmosphere and generates related information [15] [16]. Finally, the Fragmentation Analysis (FG) service provides detection and characterisation of in-orbit fragmentations, break-ups or collisions, and analyses all the available information regarding the involved object(s) [17] [18]. This last one is particularly relevant since fragmentation events, including both explosions and collisions, are currently the dominant source of space debris [19]. In this context, the timely monitoring of a on-orbit break-up and fast procedures to forecast the trajectories of resultant objects are of paramount importance. These objectives entail prior characterization of the event, to identify where and when the generated fragments propagated from the primary object.

Assigning newfound fragments to the corresponding parent is a fundamental task to mitigate the collision risk and increase the safety of newly designed space missions. To this aim, numerous procedures deriving from track-to-track association methodologies can be extended to the track-to-fragmentation case, exploiting their association and estimation techniques for an efficient and automated use of the data gathered through SST sensors [20]. Different track-to-track methods exist in the literature, which adapt to the quantity and type of information available. Focusing on angular observations, a procedure to match two uncorrelated tracks is proposed in [21]. Compressing the track with a least-squares optimization, a 4-dimensional vector called angular attributable $\mathcal{A}_{ang} = (\alpha, \delta, \dot{\alpha}, \dot{\delta})$ is obtained, extracting two angles and two angular velocities from a single angular track. Then, the algorithm exploits the Admissible Region (AR) tool to restrict the object state to lie within a two-dimensional submanifold of the measurement space, imposing orbital constraints to make up for the lack of an Orbit Determination (OD) process. Such a region can be mapped into orbital elements space and propagated in time, in order to perform an intersection in the same space with the AR associated with another angular track. This approach simplifies the orbit correlation and determination process to geometrical intersections of hyper-surfaces and it is called Intersection Theory Analysis (ITA), performing correlation without needing Initial Orbit Determination (IOD). Finally, different linkage methodologies built on the AR concept are proposed and compared in [22], to find the most efficient one in determining whether two or more observations pertain to the same objects. Here, Differential Algebra (DA) is employed together with the Automatic Domain Splitting (ADS) technique to control the truncation error introduced with the truncated power series.

The detection of both epoch and location of a fragmentation event has been widely investigated in the literature, as it allows operationally to predict the evolution of fragments clouds. In [23] the event epoch is identified through a backward propagation of each fragment of the analysed cloud. At each time step the distance between the propagated state and the centre of mass of the cloud is computed, and the event is detected where this distance reaches a minimum. In [24] the breakup time is identified within an approach to correlate known fragments with possible parent objects. To achieve this, five distance metrics are applied and investigated in terms of accuracy of the produced results. The PUZZLE algorithm [25] estimates the epoch of a fragmentation event, both in the short and long-term scenarios, through a first pruning and filtering of non-relevant TLEs, and a subsequent analysis of the orbital elements of the remaining ones. Indeed, close to the breakup event, the generated fragments present similarities in some of the Keplerian elements. Despite the ease and effectiveness of these methods, numerous ephemerides of various fragments are assumed to be known and associable to an already catalogued parent object. This facilitates the epoch estimation, but it represents a less frequently applicable assumption in a realistic operational scenario. Instead, in the context of this work, it is assumed that the estimation of fragmentation epoch is required shortly after the event is alerted, when a small number of debris ephemerides (or a single one) is known. This fundamental premise comes from the FRagmentation Epoch Detector (FRED) algorithm [26], representing the starting point for the implementation of a new routine. FRED aims to detect the epoch of a fragmentation event, exploiting one ephemeris of the parent object and a single orbital state of a generated fragment. In particular, the approach is stochastic: different distance metrics are investigated to compare the statistical distributions of Minimum Orbit Intersection Distance (MOID) and relative distances between parent and fragment. Fragmentation epoch candidates are first identified and then ranked according to the statistical distance between the two distributions. The best fragmentation epoch is finally returned in terms of mean value and standard deviation. An alternative criterion belonging to the theory of Conjunction Analysis (CA) for the ranking of the fragmentation epoch candidates has been investigated in the new approach described in this paper. CA refers to the assessment of possible in-orbit collisions between any object. If their distance falls below a certain threshold, or the PoC is sufficiently high, the collision risk cannot be neglected. The computation of the PoC is usually performed at the Time of Closest Approach (TCA). Conjunction events are commonly distinguished between long-term and short-term. The short-term conditions allow to compute

the PoC in a linear and simple way by making a series of assumptions. Therefore, short-encounter PoC methods are and leveraged in the implementation, in particular Chan's approach [27] is applied.

As mentioned up to now, considering the importance of associating promptly a fragment to a parent object and detecting the epoch in a break-up event, two new algorithms have been implemented at Politecnico di Milano. The Orbital Parameters Intersection Analysis (OPIA), dedicated to the correlation of fragments observations to breakup events, bases its innovative aspect in the use of the admissible region tool, which allows to carry out this operation without requiring any result of IOD of the fragment. The new FRED approach aims to estimate the epoch of a fragmentation event, verifying if the approach implemented in FRED can be enhanced with alternative metrics, such as the PoC measure, for the characterization of fragmentation events.

The paper is structured in the following way. Section 2 describes in details the mathematical and implementation framework of the OPIA algorithm. In section 3, the new approach based on FRED algorithm is as well presented and described in its steps. Section 4 details how the data-set of the test-case used to validate both algorithms is prepared. In section 5 the numerical and graphical results of the simulated test-case and related considerations are presented for both algorithms. Section 6 briefly shows the integrated approach developed to unify the two methods in a single tool. Finally, in section 7 the conclusions on the two approaches presented are drawn, as well as the possible future developments to investigate.

2. OPIA approach

The algorithm tailored to the association of observations to a fragmentation event is called OPIA. The method bases its foundations on the admissible region tool, which allows it to handle too-short observational arcs without OD results. The core association analysis is then performed in the orbital elements space, with particular focus on the inclination (i) and on the right ascension of the ascending node (RAAN). These parameters describing the orbital plane exhibit very slow variations due to orbital perturbations, connected to the J_2 nodal regression for the RAAN and to the third body perturbation for the inclination, and even during a fragmentation event many fragments preserve inclination and RAAN similar to those of the parent object.

2.1 Context

Let's consider the breakup of a space object orbiting around the Earth, whose blast-point state $\mathbf{x}^{blast}$ and epoch t_{blast} have already been characterized. Some hours later, at t_{obs}, one object is detected by a ground station (optical or radar), recording an angular track into a TDM. The final objective of the algorithm is to assess whether the object is associated to the detected fragmentation event.

2.2 Distributions characterization

The angular attributable of the observed object $\mathcal{A}_{ang} = (\alpha, \delta, \dot{\alpha}, \dot{\delta})$ is extracted from the angular track recorded in the TDM, and the corresponding admissible region is found and sampled at t_{obs}. Provided the observer geocentric position $\mathbf{q}^{obs}$ and velocity $\dot{\mathbf{q}}^{obs}$, the admissible attributable found are converted from measurements to Cartesian space, generating multiple Virtual Debris (VDs), and then propagated backward in time to t_{blast}. This last step can be skipped to obtain an algorithm free from the propagation process, taking advantage of the low sensitivity of inclination and RAAN to orbital perturbations to develop the same analysis described below without knowing the fragmentation epoch.
From the propagated admissible states $\mathbf{x}_i^{blast}$ it is possible to compute the Keplerian parameters of VDs at t_{blast}, whose distribution can be characterized on the (i, Ω)-plane. The shape of the distribution is described through the Gaussian (or normal) assumption, so that the sample mean $\boldsymbol{\mu}_{\mathrm{VD}}$ and covariance $\boldsymbol{\Gamma}_{\mathrm{VD}}$ can be computed.
Focusing now on the parent object state $\mathbf{x}^{blast}$ at the fragmentation epoch t_{blast}, it is possible to apply the NASA Standard Breakup Model (SBM) [28] to find the synthetic distribution of simulated fragments after the event. In this way, Virtual Fragments (VFs) states $\mathbf{x}_k^{blast}$ are retrieved and converted into the Keplerian space, obtaining the VFs inclinations and RAAN on the (i, Ω)-plane. Also in this case, the distribution is described as Gaussian and the sample mean $\boldsymbol{\mu}_{\mathrm{VF}}$ and covariance $\boldsymbol{\Gamma}_{\mathrm{VF}}$ are computed.

2.3 Association process

The correlating phase consists in evaluating the statistical distance between the two distributions found at the previous points. This is done employing the Mahalanobis distance metric, and the main steps are:

- Computation of the squared Mahalanobis distance D^2 between the distributions:

$$D^2(\boldsymbol{\mu}_{\mathrm{VD}}, \boldsymbol{\mu}_{\mathrm{VF}}) = (\boldsymbol{\mu}_{\mathrm{VD}} - \boldsymbol{\mu}_{\mathrm{VF}})^T (\boldsymbol{\Gamma}_{\mathrm{VD}} + \boldsymbol{\Gamma}_{\mathrm{VF}})^{-1} (\boldsymbol{\mu}_{\mathrm{VD}} - \boldsymbol{\mu}_{\mathrm{VF}}) \quad (1)$$

- Characterization of the χ^2 critical value for the interval of confidence set (99.8%), through the MATLAB®function `chi2inv`.
- Finally, finding the correlation index R (or coefficient) as $R = \left| \frac{D^2}{\chi^2} \right|$.

Eventually, if the computed correlation index R is below a certain threshold $R_{max} = 1$ the object is *correlated* to

the fragmentation event, otherwise the object is considered *uncorrelated*. An example of a positive correlation is depicted in Fig. 1.

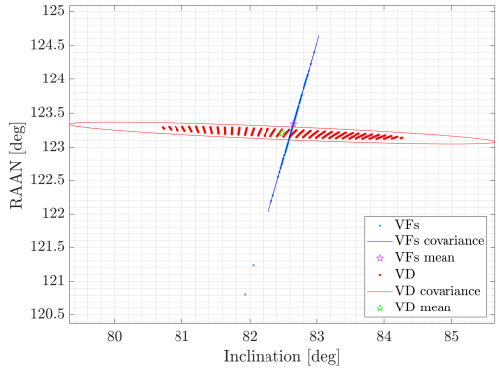

Fig. 1. Means and covariances on (i, Ω)-plane of the virtual debris and virtual fragments distributions found at t_{blast}.

As introduced previously, the algorithm works in the same way even if VDs propagation is avoided and $\boldsymbol{\mu}_{\mathrm{VD}}$ and $\boldsymbol{\Gamma}_{\mathrm{VD}}$ are found at t_{obs}, as the variations in inclination and RAAN are negligible in the time horizon considered in this analysis. For this reason, it is possible to focus on these quantities without performing the propagation step for the VDs, since their orbital parameters obtained from the admissible region at the observation epoch can be compared to the ones of the VFs at the fragmentation epoch without a relevant impact on the final outcomes, reducing in this way the computational cost.
An important implication of the comment above is that it is possible to apply the NASA SBM starting from the last parent ephemeris $\{\mathbf{x}^{eph}, t_{eph}\}$, that is without performing any propagation of the parent object to the fragmentation epoch. As consequence, it is possible to perform the implemented analysis even if the fragmentation event is not characterized. Due to the low sensitivity of these orbital parameters, the VFs distribution in the (i, Ω)-plane can be considered accurate enough even if not performed at t_{blast}.
This allows to link the fragment and the parent before the characterization of the event itself, improving and speeding up the cloud monitoring process.

3. New FRED approach

3.1 Parent covariance association

For the parent object, a covariance matrix representing the uncertainty of the state obtained from the available TLE shall be first estimated. The approach in [29] is exploited to this end. A covariance matrix and auto-correlation functions are both obtained by exploiting solely a set of publicly available TLEs in a time span of two weeks maximum. In the case of this work a number of secondary $N_{tle} = 5$ was downloaded from Space-Track and used. This approach was applied to the TLE of the specific test case. The graphic result of this covariance generation is reported in Fig. 2, showing the benefits of this shape of the parent covariance matrix. In particular, the result of the splitting phase operated through a Gaussian Mixture Model (GMM) is represented as well, both at the TLE epoch (Fig. 2a), that is when the splitting is performed, and at the alert one (Fig. 2b).

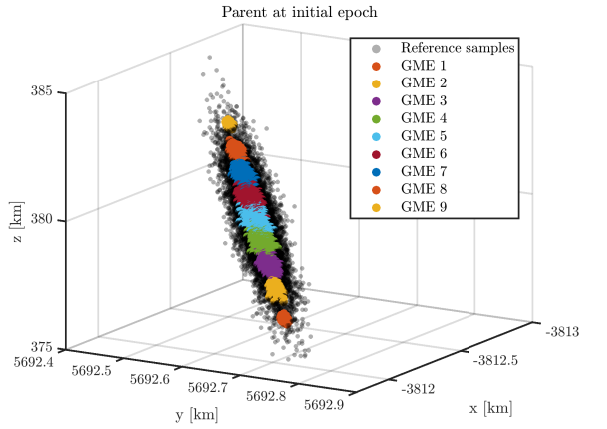

(a) Epoch t_{tle}.

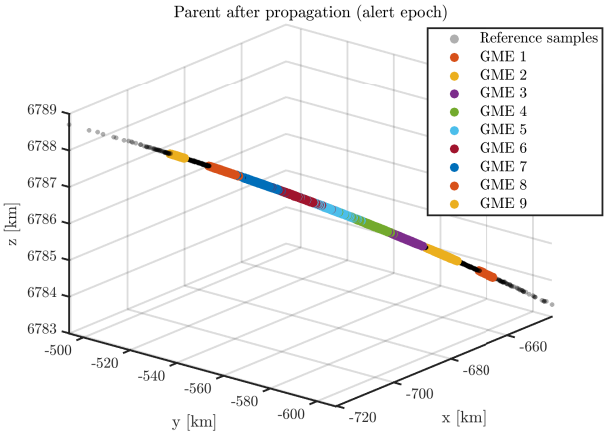

(b) Epoch t_a (alert epoch, after propagation).

Fig. 2. Parent object GMEs. Positions in ECI frame.

3.2 Candidate TCAs computation

The first block of the algorithm (Fig. 3) computes a set of candidate epochs of possible encounters for each element i_p of the parent mixture $(\{\boldsymbol{x}^p_{i_p}, \boldsymbol{P}^p_{i_p}\})$ and for each element i_f of the fragment mixture $(\{\boldsymbol{x}^f_{i_f}, \boldsymbol{P}^f_{i_f}\})$. The ephemerides of the parent object is referred to as $\boldsymbol{x}^p$ and is dated to t_{tle}, epoch of the last TLE available before the event. The covariance matrix of the parent $\boldsymbol{P}^p$ is also

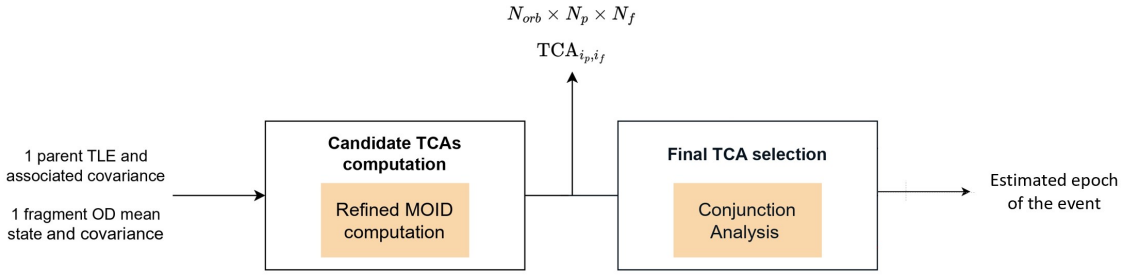

Fig. 3. New FRED approach: flow chart.

dated to t_{tle} and associated to $\boldsymbol{x}^p$ (Sec. 3.1). The event has occurred at $t_0 > t_{tle}$ and the related alert has been notified at $t_a > t_0$. Some hours later, a fragment is detected by a surveillance radar at $t_{od} > t_0$ and its mean orbital state $\boldsymbol{x}^f$ and covariance matrix $\boldsymbol{P}^f$ are computed from an OD process better detailed in Sec. 4. This first portion of the algorithm is structured as follows:

1. The window $[t_{tle}, t_a]$ is sampled with frequency $1/T_p$, T_p being the parent orbital period. This results in N_{orb} number of epochs t_i, each related to the i-th periodicity.
2. N_p and N_f Gaussian Mixture Elements (GMEs) are generated through splitting. The state vectors $\boldsymbol{x}^p_{i_p}$ with $i_p = 1, ..., N_p$ and $\boldsymbol{x}^f_{i_f}$ with $i_f = 1, ..., N_f$ are produced.
3. A nested loop is started for each parent and fragment GME.
4. The states of parent and fragment GMEs are propagated to each t_i.
5. For each t_i, the MOID distance and its transit epochs are computed analytically (following [30]) for both elements i_p and i_f, leveraging Kepler's equation. Results are referred as $t^p_{i_p,i_f}$ and $t^f_{i_p,i_f}$. The i_p and i_f state vectors are propagated up to $t^p_{i_p,i_f}$ and $t^f_{i_p,i_f}$ respectively, resulting in the orbital states $\boldsymbol{x}^p_{i_p}(t^p_{i_p,i_f})$ and $\boldsymbol{x}^f_{i_f}(t^f_{i_p,i_f})$, and the analytical computations of $t^p_{i_p,i_f}$ and $t^f_{i_p,i_f}$ are updated. Both epochs are iteratively modified in this manner until, between two consecutive steps, they do not change anymore (setting a tolerance of 1e $-$ 03 s) ([26]). This iterative process results in $N_{orb} \times N_p \times N_f$ couples of $\left(t^p_{i_p,i_f}, t^f_{i_p,i_f}\right)$ and $\left(\boldsymbol{x}^p_{i_p}(t^p_{i_p,i_f}), \boldsymbol{x}^f_{i_f}(t^f_{i_p,i_f})\right)$.
6. The fragment i_f state vector $\boldsymbol{x}^f_{i_f}(t^f_{i_p,i_f})$ is propagated up to $t^p_{i_p,i_f}$, resulting in $\boldsymbol{x}^f_{i_f}(t^p_{i_p,i_f})$.
7. To exclude unfeasible solutions, the $N_{orb} \times N_p \times N_f$ couples enter a filtering phase, applied on the epoch of parent element i_p transiting through the MOID ($t^p_{i_p,i_f}$). This is selected instead of $t^f_{i_p,i_f}$ due to the higher reliability associated to the parent state. The first filter requires that the couples with combinations (i_p, i_f) for which $t^p_{i_p,i_f}$ is not included in the boundaries of the time window $[t_{tle}, t_a]$ are eliminated. With the second filter, for each t_i, the couples with combinations (i_p, i_f) for which $t^p_{i_p,i_f} < (t_i - T_p/2)$ or $t^p_{i_p,i_f} > (t_i + T_p/2)$ are filtered out. The last filter is based on a clustering algorithm (DBSCAN), applied to eliminate couples with combinations (i_p, i_f) considered outliers (setting the maximum time deviation to 5 minutes).
8. If $t^p_{i_p,i_f}$ related to all combinations (i_p, i_f) is not compliant for all of the periodicities, the fragment under analysis must be discarded.

For the fragments which are not discarded, the epochs of the element i_p transiting through the MOID are refined, exploiting the orthogonality between the relative position and the relative velocity. The candidate TCAs are found in correspondence of a null scalar product between position and velocity, through an optimization function and applying the Keplerian model. This allows to obtain in output a set of candidate TCA epochs, in number $N_{orb} \times N_p \times N_f$. At this point each parent and fragment GME ($\{\boldsymbol{x}^p_{i_p}, \boldsymbol{P}^p_{i_p}\}$ and $\{\boldsymbol{x}^f_{i_f}, \boldsymbol{P}^f_{i_f}\}$) is propagated through an UT function to the final candidate TCAs epochs.

3.3 Final TCA selection

The second block of the algorithm (Fig. 3), aims to finally detect the fragmentation event epoch. The inputs are obtained from the first portion of the routine and are thus processed using typical metrics of collision risk assessment. The event under analysis is treated as a collision between a primary object (the parent) and a secondary object (the fragment).

$$d_M\left(\text{TCA}_{i_p,i_f}\right) = \left[\left(\boldsymbol{r}^f_{i_f}(\text{TCA}_{i_p,i_f}) - \boldsymbol{r}^p_{i_p}(\text{TCA}_{i_p,i_f})\right)\right]^T [\boldsymbol{P}^p_{i_p}(\text{TCA}_{i_p,i_f}) + ... \\ \boldsymbol{P}^f_{i_f}(\text{TCA}_{i_p,i_f})]^{-1} \left[\left(\boldsymbol{r}^f_{i_f}(\text{TCA}_{i_p,i_f}) - \boldsymbol{r}^p_{i_p}(\text{TCA}_{i_p,i_f})\right)\right] \quad (2)$$

The block is structured as follows:

1. A nested loop is started for each parent and fragment GME.
2. For each t_i, the PoC between the current parent and fragment GMEs is computed through Chan's method [27]. The distributions $\{\boldsymbol{x}^p_{i_p}(\text{TCA}_{i_p,i_f}), \boldsymbol{P}^p_{i_p}(\text{TCA}_{i_p,i_f})\}$, $\{\boldsymbol{x}^f_{i_f}(\text{TCA}_{i_p,i_f}), \boldsymbol{P}^f_{i_f}(\text{TCA}_{i_p,i_f})\}$ at the corresponding candidate TCA epochs enter in the PoC computation. The covariance matrices are required solely in their positional components. The Hard Body Radius (HBR) of the combined sphere is also required.
3. For each combination (i_p, i_f), N_{orb} collision probabilities are obtained ($P^c_{i_p,i_f}(\text{TCA}_{i_p,i_f})$). To locate a potential encounter in time, the periodicity and the corresponding TCA at which the computed probability is maximum are selected.
4. Overall, $N_p \times N_f$ TCA_{i_p,i_f} are hence obtained, retaining only those "selected" through the maximum PoC criterion. Only the couples mean-covariance corresponding to these TCA epochs are now considered.
5. A second statistical distance metric is applied. For each combination (i_p, i_f) the Mahalanobis distance is computed between the current parent and fragment GMEs as in Eq. 2, where the matrices $\boldsymbol{P}$ refer only here to the positional sub-covariance.
6. Of all $N_p \times N_f$ values of $d_M(\text{TCA}_{i_p,i_f})$, the minimum is identified. The corresponding $\tilde{i}_p$ and $\tilde{i}_f$ indexes are selected, and the related epoch $\text{TCA}_{\tilde{i}_p,\tilde{i}_f}$ is considered the final estimate $\tilde{t}_0$. This implies to obtain a solution of the event epoch which corresponds to the closest distributions from the two mixtures, in terms of position.
7. The time error of the estimated solution compared to the true fragmentation epoch is finally computed as:

$$\varepsilon = |t_0 - \tilde{t}_0| \tag{3}$$

For a single fragment analysis, the result is considered successful if error in Eq. 3 is below a threshold quantity, set equal to 60 s.

4. Test case and data-set generation

The fragmentation scenario investigated in LEO is related to the explosion of the Soviet electronic intelligence satellite COSMOS 1408 (1982-092A) [31] [32], induced by a kinetic anti-satellite test which occurred around 02:47 UTC of November 15th, 2021 [33]. The abandoned spacecraft generated a debris cloud comprising more than 1700 trackable pieces, about 1300 of which larger than 10 cm, as well as about 60,000 fragments greater than 1 cm. The event is considered to have already been characterized and the orbital parameters of the satellite at the fragmentation epoch are gathered in Table 1.

a [km]	e	i [deg]	Ω [deg]	ω [deg]	θ [deg]
6862.2	2.851e-03	82.67	123.40	91.92	341.85

Table 1. Orbital parameters of COSMOS 1408 at the fragmentation epoch.

The NASA SBM (formulation in [34]) is exploited to model the fragmentation event and generate a certain number of objects from which fictitious measurements are derived. Specifically, the SBM allows to compute the orbital states of the fragments derived from the parent object involved in the tested scenario, from Eq. 4.

$$\begin{cases} \boldsymbol{r}^f = \boldsymbol{r}^p \\ \boldsymbol{v}^f = \boldsymbol{v}^p + \Delta\boldsymbol{v}_{SBM} \end{cases} \quad \text{at } t_{event} \tag{4}$$

The superscripts p and f refer respectively to the parent and fragment objects, while $\boldsymbol{r}$ is labelled to the positional state and $\boldsymbol{v}$ to the velocity vector.
The application of the SBM to simulate the fragmentation involving COSMOS 1408 leads to the generation and dispersion of fragments that are represented in Figures 4 and 5. The output of the simulation consists of 237 virtual fragments, representing the data-set needed to test the performance of both OPIA and FRED algorithm.

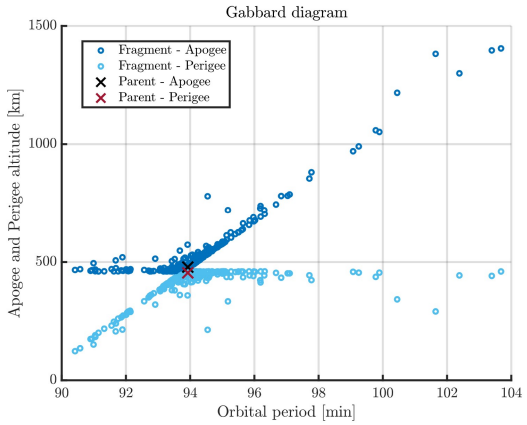

Fig. 4. Gabbard diagram of the simulated break-up event involving Cosmos 1408.

The obtained fragments ephemerides are propagated to epoch t_{obs} (obtaining $\boldsymbol{x}^f(t_{obs})$), when an observation window is simulated from a fictitious ground-station, to retrieve virtual sets of measurements feeding both OPIA and new FRED algorithms. Additionally, for the testing

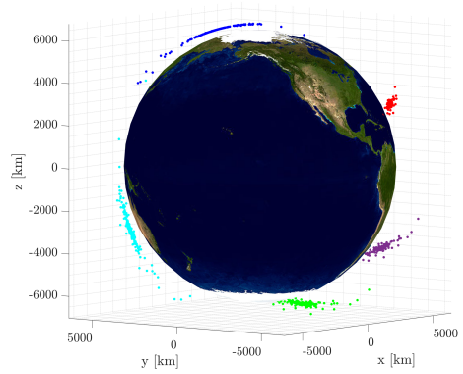

Fig. 5. Evolution of the simulated fragments cloud from COSMOS 1408. The time evolution can be followed through the colored clouds starting from the red one, after only a quarter of the period from the fragmentation, to then proceed with the purple one, the green one, the cyan one, and the blue one, after a complete period from the fragmentation.

of the new FRED approach, these measurements are processed through the application of an IOD and Refined OD (ROD) functions (with or without introducing errors on the orbital state, depending on the scenario). Thus, the final output is the couple mean state and uncertainty covariance for each single fragment, both in position and velocity ($\{\boldsymbol{x}^f, \boldsymbol{P}^f\}$).

It is worth to point out that also space objects not related to the event need to be generated to test the ability of the OPIA algorithm in avoiding wrong associations and, for this purpose, the Space-Track catalogue is exploited to obtain TLEs of generic LEO objects, represented in Fig. 6. By this way, a space object catalogue is defined and reported in Tab. 2, including both simulated fragments (from SBM) and space objects not related to the breakup (from Space-Track). OPIA numerical simulation is tested by processing this catalogue to investigate for possible correlations to an alerted fragmentation event.

Simulated Fragments	No Fragments
237	2919

Table 2. Space objects catalogue considered in the OPIA simulation. It includes both simulated fragments and objects not related to the break-up.

5. Results

5.1 OPIA

OPIA performance is tested in LEO through the dataset built in Sec. 4. The true simulated fragments generated

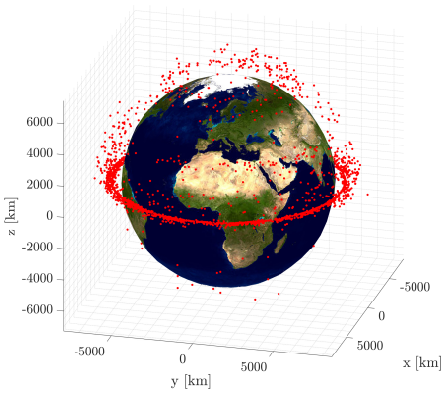

Fig. 6. LEO satellites tracked on Space-Track, employed as no-related objects.

by the fragmentation event were propagated up to 1 day after the event, to then perform the virtual measurements that allows to test the ability of the algorithm in associating observation of objects related to the fragmentation (true positives and false negatives). In the same fashion, the TLEs of objects not related to the event are acquired from the Space-Track platform the day after the fragmentation, entering in the same pipeline of the true fragments, this time to test the ability of the code in excluding false associations (false positives and true negatives). The outcomes presented in Tab. 3 do not include the propagation step since this reduces the computational cost without causing a degradation in accuracy.

Quantity	Result
True positives	99.16%
False negatives	0.84%
True negatives	100.00%
False positives	0.00%

Table 3. OPIA nominal correlation performance.

OPIA shows great accuracy and effectiveness in correlating objects in the LEO environment, where the main source of false negatives is a large component of Δv, appreciable from the degradation of the correlation index as a function of the velocity change magnitude in Fig. 7.

In LEO, it is also interesting to observe the distribution of the correlation coefficients with respect to the RAAN of the correlated fragments in Fig. 8, reproducing the quadratic behavior imposed by the χ^2-test and expressed in Eq. 1. Fragments with RAAN closer to the parent ones present a smaller correlation index, favoring the association process.

While the code demonstrates excellent performance in the LEO environment, it is fundamental to acknowledge

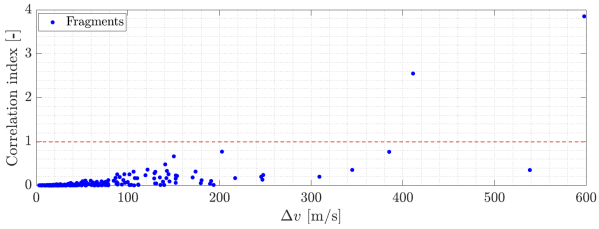

Fig. 7. Correlation index distribution as a function of the velocity change between true fragments and parent object in LEO, together with the association threshold $R_{max} = 1$.

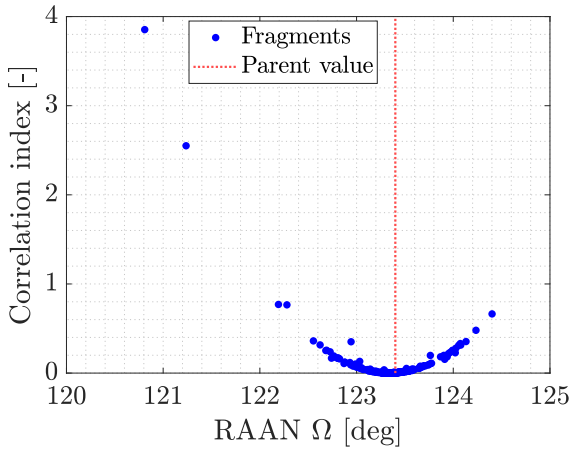

Fig. 8. Correlation index distribution as a function of the real fragments RAAN in LEO.

potential challenges when applying this type of analysis to the Geostationary environment. In GEO, the objects tend to have very similar orbital inclinations, which can complicate the analysis based on orbital inclination and RAAN like the one implemented in OPIA.

5.2 New FRED

The same data set is then tested with the new FRED algorithm. First of all, it is necessary to define the criteria for considering a result as wrong. For all fragments that do not yield a correct estimation ($\varepsilon > 60$ s), two categories can be identified. In the *periodicity failures* case, at least one combination (i_p, i_f) leads to find the highest PoC value outside of the correct periodicity (in this case the third one), resulting in ε larger than half of the parent orbital period. In the *TCA failures* case, even though convergence to the correct periodicity is achieved for all combinations (i_p, i_f), the error is anyway higher than a minute. This can be attributed to a less accurate estimation of the candidate TCA epochs, and may occur in the MOID computation or in the afterward refinement of the TCAs.

5.2.1 Scenario with no OD error

The unperturbed scenario without OD error is first tested to assess the theoretical performance of the routine. The propagation in time, both in the dataset generation and within the algorithms, occurs here through an analytical Keplerian model. The fragments detection and subsequent OD process is conducted with no error. In this case 229 fragments "survived" all filters; their results are reported in Tab. 4. All fragments estimate the event epoch

Case	Correct solutions	Periodicity failures	TCA failures
Kep	100%	0%	0%
SGP4	100%	0%	0%

Table 4. Results for the scenarios with no OD error.

with an error of less than a minute, even in the order of milliseconds. This is illustrated by the cumulative error ε, which is reported in absolute value and in seconds in Fig. 9.

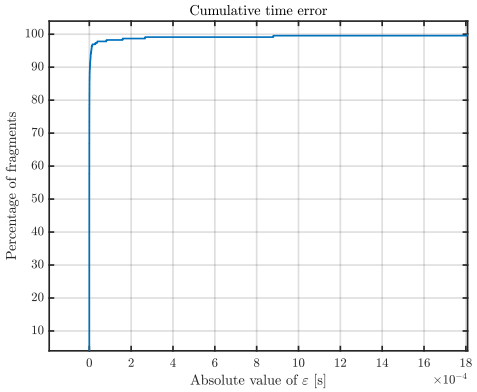

Fig. 9. Cumulative time error ε in the unperturbed scenario with no OD error.

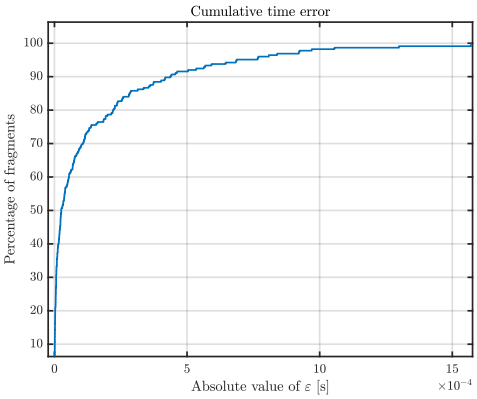

Fig. 10. Cumulative time error ε in the perturbed scenario with no OD error.

The same remarkable performance are obtained in the perturbed scenario (results in Tab. 4 and Fig. Fig. 10). The conversion inside SGP4 function from the Cartesian to TEME frame (and viceversa) is performed through a fixed-point iteration loop, introducing possible numerical errors. However in this case it does not affect significantly the outcome in terms of correctness of the solution, while the measurements noise will have the most significant impact.

5.2.2 Scenario with OD error

The routine shall be tested under conditions that are as representative as possible of an operational scenario, for which it is necessary to introduce an error. This results in a perturbation of the fragments mean orbital state with respect to the state referred to as ground-truth. Therefore, their detection is performed here through the approach described in Sec. 4, introducing an error in the OD process through the measurements noise covariance. The results of the new FRED algorithm are reported for both the perturbed and unperturbed cases in Tab. 5. As evident, in the majority of cases, the algorithm successfully converges to the correct solution. Yet, upon comparing results in Tab. 4 with those in Tab. 5, it is evident that the discrepancy introduced in the OD significantly impacts the algorithm performance, particularly in terms of the highest PoC metric. The latter fails in placing the event occurrence inside the correct periodicity more times than the refined MOID computation in deriving accurate candidate TCAs. This is reflected as well in the cumulative error graphs, reported in absolute value and in minutes (Fig. 11 and Fig. 12).

Case	Correct solutions	Periodicity failures	TCA failures
Kep	82.5%	17.0%	0.5%
SGP4	83.1%	16.9%	0%

Table 5. Results for the scenarios with OD error.

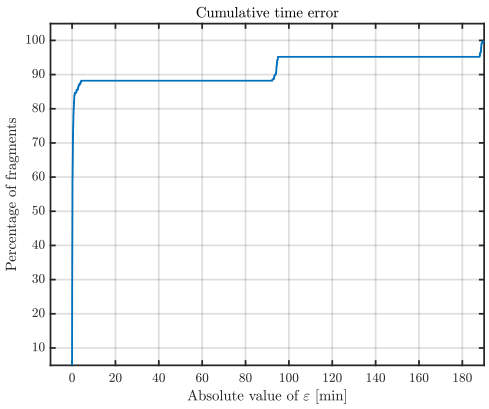

Fig. 11. Cumulative time error ε in the unperturbed scenario with OD error.

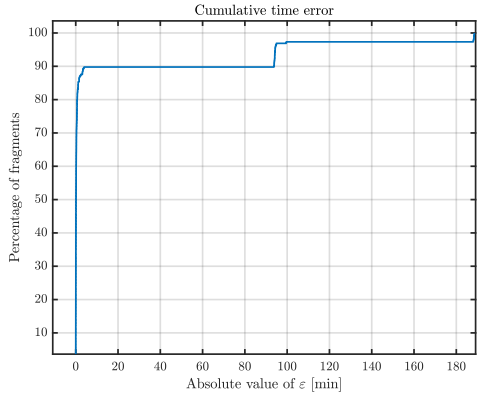

Fig. 12. Cumulative time error ε in the perturbed scenario with OD error.

As showed in Tab. 5, the number of correct solutions obtained when using SGP4 does not worsen with respect to the unperturbed case, as one may expect. Indeed, it is true that in the perturbed case errors due to the conversion from SGP4 to Keplerian elements are introduced. However, it could happen that these errors offset those caused by OD noise. In such a case, if state errors would lead to the selection of the wrong periodicity through the PoC metric, SGP4 conversion errors instead could simultaneously guide the algorithm to the correct periodicity.

6. Integrated approach

From an operational point of view, a tool that can both associate the input fragment to the parent object and detect the epoch of a fragmentation event has been investigated. In particular, an integrated approach, highlighting the complementary nature of both OPIA and new FRED methods, is proposed and represented in Fig. 13. Let's assume a fragmentation event has occurred and is alerted but not yet characterized. Assuming that the last TLE or OD result of the parent object(s) involved is available at an epoch previous to the event (1), as well as a set of TDMs recorded through the observations of possible fragments (2), the OPIA algorithm is first run to verify which of those TDMs are related to objects produced within the event (3). Notice that this first step is performed without having computed the epoch of the fragmentation yet, but relying only on the epoch of the last parent TLE. If OPIA confirms the association of a certain fragment, its measurements are processed by an OD algorithm (4) to obtain the fragment orbital state, also contributing to the cataloguing process of the debris. Afterwards, the OD informations are provided to the new FRED algorithm (5), which finally characterizes the event in terms of epoch and location computation. The knowledge of the event epoch and location is then employed for planning new fragments observations, obtaining more reliable TDMs and as a con-

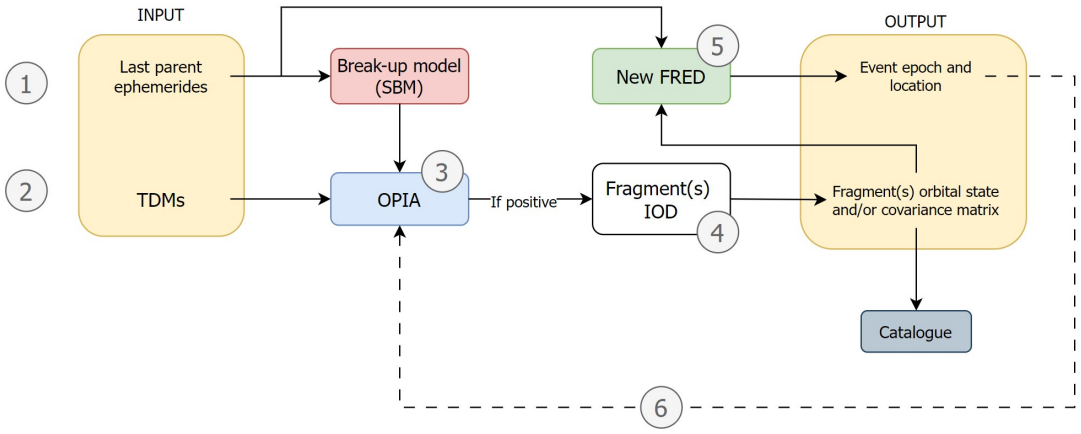

Fig. 13. Possible integration of OPIA and new FRED approaches for operative application.

sequence, improving OPIA performance on future detections (6) and the catalogue screening of objects generated during the event.

7. Conclusions and future developments

7.1 Conclusions

This paper presents two approaches developed in the SST context to enhance a prompt characterization of break-up events, occurring around the Earth. The first one, OPIA, performs the association of an observed object to the fragmentation event. The other, an upgrade of the previously implemented FRED algorithm, estimates the epoch of a fragmentation event.

OPIA bases its track-to-fragmentation process on the admissible region formulation, which allows to handle very short observational arcs, even where the classical methods for IOD fail. The most innovative aspect lies precisely in the association process, which can be performed even without determining the orbit of the fragment. OPIA exploits the similarity of inclination and RAAN of the admissible region samples and guarantees excellent accuracy in LEO, but may present deteriorated performance in GEO, as the similarity between the above-mentioned orbital parameters in the objects catalogue lead to many false associations.

The new FRED algorithm is able to detect the epoch of a fragmentation event, exploiting a single fragment orbital state and one ephemeris of the fragmented object. Statistical metrics typical of CA, such as the Mahalanobis distance and the PoC, serve to detect first the interval where the event could have possibly occurred, and secondly the precise resulting epoch. The uncertainties in the knowledge of the orbital states of both parent and fragment objects is introduced and propagated using a GMM based approach. The latter allows to increase reliability in the stochastic representation with respect to propagating a single Gaussian covariance, meanwhile decreasing the computational effort required by a Montecarlo approach. Regarding the presented results, the approach operates with a one hundred percent success rate if the scenario conditions are close to being ideal. Instead, when introducing perturbations, the results do not experience any degradation if again no error is applied in the OD. This is a positive outcome; however, numerical errors resulting from the conversion to SGP4 elements are reflected in the epoch estimates. These are still in the order of milliseconds far from the actual epoch, but deviate slightly more than in the Keplerian case. In cases where the dataset is generated with OD errors, the majority of "failed" simulations are attributed to the lack of convergence through the PoC computation, rather than to an inaccurate evaluation of TCA epochs. Moreover, convergence to the correct periodicity through the maximum PoC criterion, which in most cases determines a final error below a minute, is affected by high uncertainties and errors in the fragment states.

Finally, an integrated approach has been presented to characterize a single functional module, representing a solid tool dedicated to the early characterization of a fragmentation event.

7.2 Future developments

The potential of the OPIA algorithm could lead to developments beyond the simple fragment-event association: with a time-variant analysis, it would be interesting to investigate if this tool can prove to be a basis for algorithms dedicated to the characterization of fragmentation epoch and location, as done in FRED, but starting from a single fragment observation and without IOD results.

Regarding the new FRED approach, the method lacks the ability to output statistical information (mean value and standard deviation), providing a single estimate of

the epoch. Thus, a next crucial step involves the study of higher-order moments beyond the mean and variance, whose relevance is limited to Gaussian distributions. Furthermore, future research may focus on introducing existing methods of CA that inherently address the dilution problem (underestimation of the PoC for high positional uncertainties).

Acknowledgements

This research has received funding as part of the work developed for the agreement n. 2023-37-HH.0 for the project "Attività tecnico-scientifiche di supporto a C-SSA/ISOC e simulazione di architetture di sensori per SST", established between the Italian Space Agency (ASI) and Politecnico di Milano (POLIMI).

References

[1] Space debris by the numbers. https://www.esa.int/Space_Safety/Space_Debris/Space_debris_by_the_numbers, accessed: 2024-07-01.

[2] Bianchi G, Bortolotti C, Roma M, Pupillo G, Naldi G, Lama L, Perini F, Schiaffino M, Maccaferri A, Mattana A, Podda A, Casu S, Protopapa F, Coppola A, Di Lizia P, Purpura G, Massari M, Montaruli MF, Pisanu T, Schirru L, Urru E. Exploration of an innovative ranging method for bi-static radar, applied in LEO Space Debris surveying and tracking. *Proceedings of the International Astronautical Congress, IAC*, 2020, 2020-October.

[3] Bianchi G, Naldi G, Fiocchi F, Di Lizia P, Bortolotti C, Mattana A, Maccaferri A, Magro A, Roma M, Schiaffino M, Cattani A, Cutajar D, Pupillo G, Perini F, Facchini L, Lama L, Morsiani M, Montaruli MF. A new concept of bi-static radar for space debris detection and monitoring, 2021, doi:10.1109/ICECCME52200.2021.9590991.

[4] Montaruli MF, Facchini L, Lizia PD, Massari M, Pupillo G, Bianchi G, Naldi G. Adaptive track estimation on a radar array system for space surveillance. *Acta Astronautica*, 2022, doi:https://doi.org/10.1016/j.actaastro.2022.05.051.

[5] Bianchi G, Montaruli MF, Roma M, Mariotti S, Di Lizia P, Maccaferri A, Facchini L, Bortolotti C, Minghetti R. A new concept of transmitting antenna on bi-static radar for space debris monitoring. *International Conference on Electrical, Computer, Communications and Mechatronics Engineering, ICECCME 2022*, 2022, doi:10.1109/ICECCME55909.2022.9988566.

[6] Bianchi G, Mariotti S, Montaruli M, Lizia PD, Massari M, De Luca M, Demuru R, Sangaletti G, Mesiano L, Boreanaz I. The new transmitting antenna for BIRALES. *Materials Research Proceedings*, 2023, 37: 474 – 477, doi:10.21741/9781644902813-104, all Open Access, Hybrid Gold Open Access.

[7] Montaruli MF, Di Lizia P, Tebaldini S, Bianchi G. Delta-k approach for space surveillance multireceiver radars. *Astrodynamics*, 2024, doi:https://doi.org/10.1007/s42064-024-0217-5.

[8] Montaruli MF, De Luca MA, Massari M, Bianchi G, Magro A. Operational Angular Track Reconstruction in Space Surveillance Radars through an Adaptive Beamforming Approach. *Aerospace*, 2024, 11(6), doi:10.3390/aerospace11060451.

[9] Montaruli M, Di Lizia P, Tebaldini S, Bianchi G. Adaptive track approach for multiple sources scenarios during radar survey for space surveillance applications. *Aerospace Science and Technology*, 2024: 109307, doi:https://doi.org/10.1016/j.ast.2024.109307.

[10] Pastor A, Escribano G, Sanjurjo-Rivo M, Escobar D. Satellite maneuver detection and estimation with optical survey observations. *Journal of the Astronautical Sciences*, 2022, 69(3): 879 – 917, doi:10.1007/s40295-022-00311-5.

[11] Cordelli E, Vananti A, Schildknecht T. Analysis of laser ranges and angular measurements data fusion for space debris orbit determination. *Advances in Space Research*, 2020, 65(1): 419 – 434, doi:10.1016/j.asr.2019.11.009.

[12] Montaruli MF, Purpura G, Cipollone R, De Vittori A, Facchini L, Di Lizia P, Massari M, Peroni M, Panico A, Cecchini A, Rigamonti M. An orbit determination software suite for Space Surveillance and Tracking applications. *CEAS Space Journal*, 2024, doi:10.1007/s12567-024-00535-1.

[13] EU Space Surveillance and Tracking: About Us. https://www.eusst.eu/about-us/, 2023.

[14] Bonaccorsi S, Montaruli MF, Di Lizia P, Peroni M, Panico A, Rigamonti M, Del Prete F. Conjunction Analysis Software Suite for Space Surveillance and Tracking. *Aerospace*, 2024, 11(2), doi:10.3390/aerospace11020122.

[15] Pardini C, Anselmo L. Impact of the time span selected to calibrate the ballistic parameter on spacecraft re-entry predictions. *Advances in Space Research*, 2008, 41(7): 1100–1114, doi:https://doi.org/10.1016/j.asr.2007.11.013.

[16] Cipollone R, Montaruli M, Faraco N, Di Lizia P, Massari M, De Vittori A, Peroni M, Panico A, Cecchini A. A re-entry analysis software module for Space Surveillance and Tracking operations. *Proceedings of the International Astronautical Congress, IAC*, 2022, 2022-September.

[17] Mains D, Peterson G, McVey J, Maldonado J, Sorge M. Forensic analysis of recent debris-generating events. *Journal of Space Safety Engineering*, 2024, doi:https://doi.org/10.1016/j.jsse.2024.06.006.

[18] EU Space Surveillance and Tracking: Services. `https://www.eusst.eu/services/`, 2023.

[19] Office ESD. ESA's Space Environment Report 2023. Technical report, ESA ESOC, Robert-Bosch-Strasse 5 D-64293 Darmstadt Germany, 2023.

[20] Pastor A, Sanjurjo-Rivo M, Escobar D. Track-to-track association methodology for operational surveillance scenarios with radar observations. *CEAS Space Journal*, 2023, 15, doi:10.1007/s12567-022-00441-4.

[21] Maruskin J, Scheeres D, Alfriend K. Correlation of Optical Observations of Objects in Earth Orbit. *Journal of Guidance, Control, and Dynamics*, 2009, doi:10.2514/1.36398.

[22] Pirovano L, Armellin R, Siminski J, Flohrer T. Data association for too-short arc scenarios with initial and boundary value formulations. *Celestial Mechanics and Dynamical Astronomy*, 2019.

[23] Andrișan RL, Ioniță AG, González RD, Ortiz NS, Caballero FP, Krag H. Fragmentation event model and assessment tool (fremat) supporting on-orbit fragmentation analysis. In *Proceedings of the 7th European Conference on Space Debris*, 2017.

[24] Dimare L, Cicalò S, Rossi A, Alessi EM, Valsecchi GB. In-orbit fragmentation characterization and parent bodies identification by means of orbital distances. In *First International Orbital Debris Conference*, volume 2109, 2019, 6007.

[25] Muciaccia A, Romano M, Colombo C, et al.. Detection and characterisation of in-orbit fragmentations over short and long periods of time. In *INTERNATIONAL ASTRONAUTICAL CONGRESS: IAC PROCEEDINGS*, 2021, 1–11.

[26] Montaruli MF, Lizia PD, Cordelli E, Ma H, Siminski J. A stochastic approach to detect fragmentation epoch from a single fragment orbit determination. *Advances in Space Research*, 2023, doi:https://doi.org/10.1016/j.asr.2023.08.031.

[27] Chan FK. *Spacecraft collision probability*, American Institute of Aeronautics and Astronautics, Inc.2008.

[28] Johnson N, Krisko P, Liou J, Anz-Meador P. NASA's New Breakup Model of Evolve 4.0. *Advances in Space Research*, 2001, 28: 1377–1384.

[29] Osweiler VP. Covariance estimation and autocorrelation of NORAD two-line element sets, 2006.

[30] Gronchi GF. On the Stationary Points of the Squared Distance between Two Ellipses with a Common Focus. *SIAM Journal on Scientific Computing*, 2002, 24(1): 61–80, doi:10.1137/S1064827500374170.

[31] EUSST. EUSST confirms the fragmentation of space object COSMOS 1408, 2021.

[32] Muciaccia A, Facchini L, Montaruli MF, Purpura G, Detomaso R, Colombo C, Massari M, Di Lizia P, Di Cecco A, Salotti L, Bianchi G. Radar observation and recontruction of Cosmos 1408 fragmentation. *Journal of Space Safety Engineering*, 2023, doi:https://doi.org/10.1016/j.jsse.2023.11.006.

[33] Muciaccia A, Facchini L, Montaruli M, et al GP. Observation and analysis of Cosmos 1408 fragmentation. *73rd International Astronautical Congress (IAC)*, 2022.

[34] Johnson NL, Krisko PH, Liou JC, Anz-Meador PD. NASA's new breakup model of EVOLVE 4.0. *Advances in Space Research*, 2001, 28(9): 1377–1384.